RECENT RESULTS AND OPPORTUNITIES AT THE IOTA FACILITY *

A. Romanov[†], D. R. Broemmelsiek, K. Carlson, D. J. Crawford, N. Eddy, D. R. Edstrom,
J. Jarvis, V. Lebedev, S. Nagaitsev, J. Ruan, J. K. Santucci, V. Shiltsev, G. Stancari,
A. Valishev, A. Warner, Fermilab, IL, USA
Y.-K. Kim, N. Kuklev, I. Lobach, University of Chicago, IL, USA
S. Chattopadhyay, S. Szustkowski, Northern Illinois University, IL, USA

Abstract

The Integrable Optics Test Accelerator (IOTA) was recently commissioned as part of the Fermilab Accelerator Science and Technology (FAST) facility. The IOTA ring was briefly operated with electrons at 47 MeV followed by a 6-months run with 100 MeV electrons. The main goal of the first run was to study beam dynamics in the integrable lattices with elliptical nonlinear magnets and in the quasi-integrable case with profiled octupole channel. The flexibility of the IOTA ring allowed a wide range of complementary studies, such as experiments with a single electron; studies of fluctuations in undulator radiation and operation with low emittance beams. Over the next year the proton injector will be installed and two runs carried out. One run will be dedicated to the refinement of nonlinear experiments and another will be dedicated to the proof-of-principle demonstration of Optical Stochastic Cooling.

INTRODUCTION

The Integrable Optics Test Accelerator (IOTA), together with the FAST superconducting linac, is an accelerator research facility dedicated to the accelerator science studies for future intensity-frontier machines. IOTA is a storage ring with perimeter of 40 meters, which can operate with beams at momentum between 50 and 200 MeV/c. The main goal of IOTA is to demonstrate the advantages of nonlinear integrable lattices [1] for high-intensity beams and to demonstrate new beam cooling methods [2]. The first experiments were conducted with readily available electrons from the FAST superconducting linac [3–12]. The high flexibility of the linac made it easy to adjust the energy and intensity of the electron beam and match the beam envelope with IOTA. Another advantage of the electron beam in IOTA is its small transverse size and natural cooling due to synchrotron radiation. This allows the use of a wider range of diagnostic tools and provides more accurate measurements compared to proton beams. Research with high intensity proton beams will begin after the completion of the proton source and the corresponding injection line.

The main parameters of the IOTA ring are listed in Table 1. Figure 1 and Figure 2 show the schematic structure and panoramic view of the ring.

Table 1: IOTA Parameters with e-beam

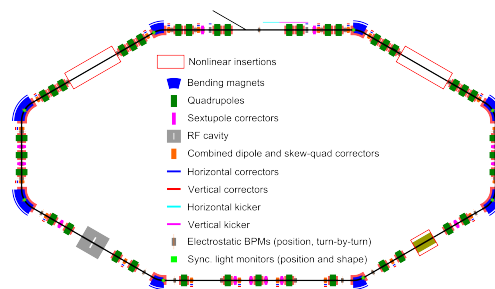| Parameter	Value
Perimeter	39.97 m
Momentum	50-200 MeV/c
Electron current	0-4.8 mA
Proton current	10 mA
RF frequency	30 MHz
RF voltage	1 kV
ν_x, ν_y, ν_s	$(0.3, 0.3, 5.7 \times 10^{-4})$
τ_x, τ_y, τ_s	(2.0, 0.7, 0.3) s
$\epsilon_x, \epsilon_{x,y coupled}$, RMS	(96.3, 25.3) nm
$\Delta p/p$, RMS	1.26×10^{-4}

Figure 1: Schematic diagram of the IOTA ring.

IOTA COMMISSIONING

Activities during the commissioning of IOTA can be divided into two groups. Firstly, the general mechanical integrity was checked and live tests of the main subsystems were carried out. During the initial period, special attention was paid to verifying the correct integration of IOTA equipment with the controls system, the correct timing of the kickers and the phasing of the RF generator with respect to the injected beam, basic BPM performance tests and minor operational improvements. The second group covers tuning the magnetic lattice of IOTA using beam-based methods and improvements to the corresponding subsystems that were necessary for the precise control of the beam dynamics.

The first IOTA run started with electron beams with momentum of 47 MeV/c and without an RF cavity in the ring due to issues with the FAST linac and ring RF. The goal of the 47 MeV program was to verify that all key IOTA subsystems are working properly by demonstration of beam circulation in the ring. Shortly after achieving these goals, both problems were resolved and run continued with electrons with a momentum of 100 MeV/c.
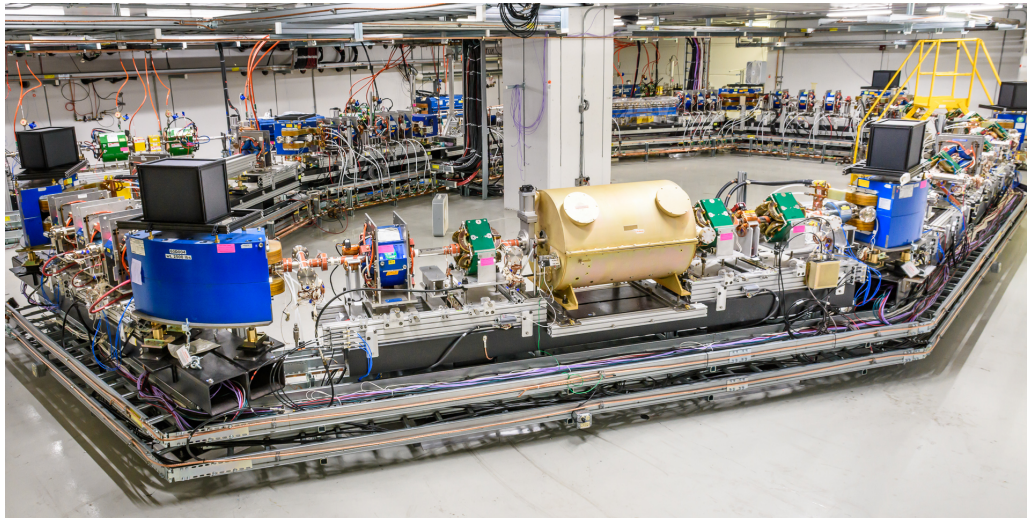
Figure 2: IOTA ring.

In both cases, the following steps were taken to inject beam into IOTA. The first revolution was traced manually according to the BPM readings. To do that, correctors in the dipoles were mainly used due to the good alignment of the elements and the relatively short circumference. Then, the LOCO algorithm was used to correct the IOTA lattice, considering it as an extension of the FAST linac. With the improved agreement between the model and the actual ring configuration, a model-dependent orbit correction was performed. This made it possible to get beam on a closed orbit that fitted within the IOTA aperture. The last step that resulted in a betatron capture was another round of LOCO lattice correction based on response data from 2 consecutive turns. Successful beam storage was obtained after scanning the RF frequency and the RF phase.

During a short shutdown over the winter holidays, four sextupoles and special vacuum chamber with 1" diameter were installed. This pipe with a smaller diameter was necessary for experiments with undulator radiation. During the continued run, a permanent magnet undulator with an adjustable gap was installed on the rails so that it could be quickly moved in and out of the beam line to avoid interference with other experiments. When experiments with non-linear insertions resumed, it was discovered that the installation of the new vacuum chamber resulted in an unexpected decrease in the mechanical aperture.

Most of the experiments were carried out with uncurrected natural chromaticity of the ring to avoid additional nonlinearities that could interfere with the studied effects. Without the chromaticity compensation, accurate measurements of betatron tunes are difficult, since the dipole oscillations of the kicked beam quickly decohere due to the natural energy spread in the electron beam. Special non-linear insertions further reduce the decoherence time. As a result, betatron tunes have been obtained from 100-300 turns. To improve the accuracy of the tune measurement, several algorithms were implemented for online and offline calculations based on data from all available BPMs. As a result, the accuracy of the measured tunes was on the order of several units of 10^{-4}. The reliable but low precision FFT algorithm was complemented by direct functional fit and primary component analysis.

During the run, continuous efforts were directed towards the improvement of precision of the turn-by-turn beam position measurements. Improvements of electronics have been supplemented by the increased beam current. Initially, the maximum stored current was limited at about 1 mA because of a longitudinal instability driven by high-order modes in the RF cavity. To suppress this, the RF damper was quickly designed and installed. As a result, it became possible to store the beam current of up to 4.5 mA, which is almost 4 times higher than the design current of 1.2 mA.

EXPERIMENTAL PROGRAM OF THE FIRST IOTA RUN

Experiments with Non-linear Magnet

The key goal of this experimental run was to demonstrate loseless operation with large nonlinear betatron tune detuning with amplitude using a special elliptic-potential magnet [1, 13]. A vertical kicker [14] pulse was varied to change the amplitude of a 100 MeV electron beam. Twenty-one beam position monitors recorded the centroid of the beam, allowing for tune-shift measurements.

The largest observed tune shift during this run was $\Delta Q_y = 0.053 \pm 0.0018$ (Figure 3). This result was measured at a nonlinear potential strength of t = 0.43 and maximum vertical kick amplitude at the non-linear insertion center of 3.65 mm. The measurements are in good agreement with MAD-X simulation with the 6 mm mechanical restriction in the undulator section of IOTA. Without the restriction the model predicts a tune shift of $\Delta Q_y = 0.085$, corresponding to an amplitude of 5.19 mm at the center of the nonlinear magnet.
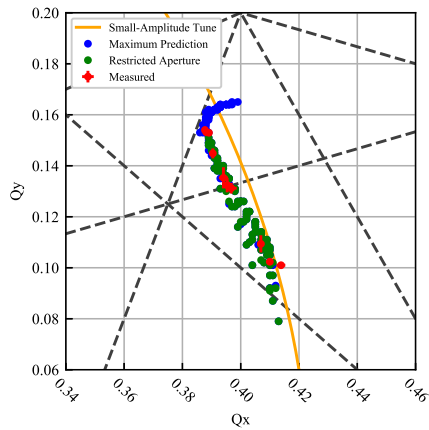
Figure 3: Tune diagram at t = 0.43, comparing measured results with simulation.

Due to mechanical restriction the full dynamical aperture could not be explored, thus a replacement for this beam pipe is in progress. Reduction of the main dipole power supply ripple and upgrade for higher precision electronics for the BPMs will be completed during shutdown. That will allow LOCO corrections to reach precision of the beta-functions beating in arcs to be within 3% and below 1% in the non-linear insertions. Further exploration of the dynamic aperture using a 150 MeV electron, pencil-like, beam will be performed using both the horizontal and vertical kickers. These improvements will enable studies of conservation of the two motion invariants in IOTA with the nonlinear magnet.

Experiments with Octupole String

Extensive studies of the non-linear beam dynamics were done with a simplified insertion device implemented as a channel of 17 discrete, individually controllable octupole magnets. Such a system can provide one invariant of motion, corresponding to octupole-type Henon-Heiles potential. This quasi-integrable (QI) setup has lower maximum tune spread as compared to the fully integrable case, but is robust and less sensitive to lattice errors by an order of magnitude while maintaining all key NIO features and requirements, thus also serving as a research platform.

Run 1 QIO studies focused on single-particle dynamics. Measurements were performed with 'pencil-like' 100MeV electron beam excited to high betatron amplitudes using a pair of single-turn kickers. From intensity and turn-by-turn beam position monitor (BPM) data, tune shift, dynamic aperture, and transverse phase space were recovered. All results followed expected scaling, with maximum achieved tune shift at DA limit being 70% of ideal simulated case (Figure 4). Invariant conservation was found to be good for several hundred turns, limited by the resolution of the BPM system and strong signal decoherence. Performance in excess of that achievable with single equivalent octupole

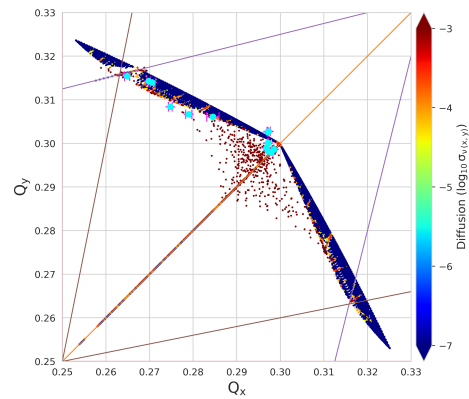was demonstrated, confirming advantageous effects of the QIO lattice.

Figure 4: Tune diagram for octupoles.

For run 2, many improvements in instrumentation are expected that will enable better BPM data and improved accuracy of linear optics, allowing for advanced studies such as particle behaviour and loss near stochastic boundaries and low-order resonances of QIO lattice. In preparation, we are performing an extensive simulation campaign to re-optimize magnet distribution for experimentally measured lattice, and study the interplay of chromaticity correction, optics tolerances, working point, and other parameters with the aim to design and train a nonlinear online correction model integrated with base LOCO tuning [15, 16].

Experiments with Anti-damper

The goal of the experiment was to demonstrate suppression of coherent transverse beam instabilities by using the non-linear focusing of the octupole strings. A transverse beam feedback system (damper) was implemented to provide a controlled method to mimic a coherent beam instability. Traditional dampers are negative feedback systems used for suppression of beam oscillations resulting from coherent beam instabilities. For this experiment, the phase of the feedback was shifted by 180° to produce positive feedback or anti-damping.

The transverse damper system consists of a beam position monitor (BPM) pickup, a pre-amplifer right at the pickup, a BPM analog module, difference amplifier, one turn notch filter, high power radio frequency (RF) amplifier, and strip line kicker.

Experimental data was collected by setting the system up in anti-damping mode with zero gain so that the beam remained stable. The system gain is then changed from zero to the desired value. The gain was increased in 1db increments until a fast instability is observed for which the gain and total beam loss was recorded. The horizontal beam size was monitored via the sync light system and was required to be the nominal $170\mu m$ or better before inducing the instability. This procedure was repeated for a variety of beam intensities with the octupoles off (0A) and on (2A). The gain threshold required to induce an instability with the octupoles
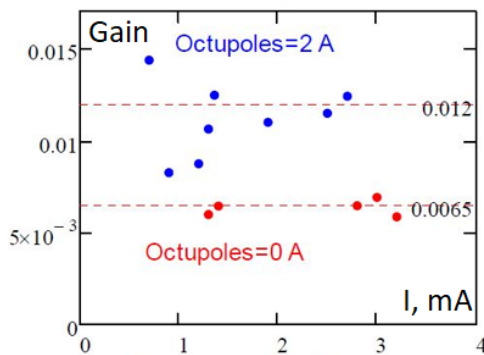
Figure 5: The measured gain threshold for induced instabilities with octupoles on and off.
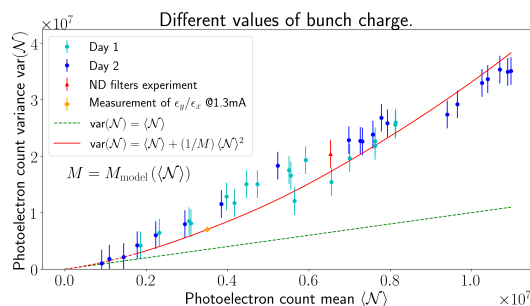

Figure 6: Photoelectron count variance var($\mathcal{N}$) as a function of photoelectron count mean $\langle \mathcal{N} \rangle$ for undulator radiation in IOTA depending on the number of electrons in the bunch.

on at 2A is double that required with the octupoles off. This demonstrates a factor of two increase in the stable region with the octupoles on (Figure 5).

While the overall expected effect of the octupoles was observed, further study is needed to characterize and understand the observed instabilities. In particular more statistics and further analysis of the fast response and growth rate measurements is needed. Implementing a digital control feedback board into the system will provide better mechanisms to collect data during instabilities, control gain, and provide the ability to make closed loop transfer function measurements of the machine to further study the stability diagram and provide means to measure chromaticity from the upper and lower sideband widths. A detailed report on this experiment can be found in [17].

Intensity Fluctuations in Undulator Radiation

The goal of this experiment was to study fluctuations of the undulator radiation [18, 19], similarly to [20]. We installed an undulator [21], which was borrowed from SLAC, into the IOTA storage ring, and used an InGaAs PIN photodiode to convert the light near the fundamental ($\lambda_1 = 1077$ nm) harmonic into photocurrent. The light was focused on the sensitive area of the photodiode with one lens, no spectral filters were used. Then, a simple op-amp based RC integrating circuit was build to integrate the photocurrent pulses, coming from the photodiode. The number of photoelectrons

$\mathcal{N}$, produced in the photodiode by one undulator radiation pulse, was inferred from the amplitude of the output signal of the integrator.

During our studies, we collected intensities for $\sim 11\,000$ turns and computed variance in the number of photons, var($\mathcal{N}$) = $\langle \mathcal{N}^2 \rangle - \langle \mathcal{N} \rangle^2$. To minimize the noise of digitization we used a comb filter with a delay equal to one IOTA revolution, and a special noise subtraction algorithm, see [18,19]. This procedure was repeated for different values of experiment parameters, and var($\mathcal{N}$) was studied as a function of these parameters. In particular, we could keep bunch charge in IOTA the same and put different neutral density filters in front of the photodiode to vary $\langle N \rangle$; also, we could remove the neutral density filters and vary the bunch charge to change $\langle \mathcal{N} \rangle$ (see Figure 6).

The variance of the number of photoelectrons for any incoherent synchrotron radiation is given by [22]

$$\text{var}(\mathcal{N}) = \langle \mathcal{N} \rangle + \frac{1}{M} \langle \mathcal{N} \rangle^2, \qquad (1)$$

where M is the number of coherent modes (see [22]). The first contribution in Eq. (1) comes from the discrete quantum nature of light, the second contribution comes from the interference of radiations of different electrons. The parameter M depends on the shape and dimensions of the electron bunch, on the type of synchrotron radiation (undulator, wiggle, bending magnet, etc.), and also on the details of light detection (accepted angle, spectral sensitivity). The exact equation for M for a Gaussian bunch was derived in [18].

Due to intrabeam scattering the electron bunch dimensions in IOTA increase with increasing the bunch charge. We measured $\sigma_x, \sigma_y, \sigma_z$ in the undulator only for one value of beam current $I = 1.3$ mA ($\langle \mathcal{N} \rangle = 3.5 \times 10^6$). The electron bunch dimensions at other values of beam current were calculateb by using a model of intrabeam scattering in IOTA, see [18]. Then, using the equation for M from [18] and Eq. (1), the theoretical prediction for var($\mathcal{N}$) (red solid lines) in Fig. 6 was obtained. It agrees with the experimental data reasonably well, and we expect to achieve better agreement when we get better at characterizing the beam in IOTA.

Experiments with Single and Few Electrons

The unique IOTA capabilities allow to analyze the behaviour of electron beams with intensities down to a single electron basing on synchrotron radiation from bending magnets. Photo Multiplier Tubes were used to register the total beam intensity together with the arrival time. In the case of a single electron, this allows us to track the evolution of its synchrotron oscillations [23, 24].

The high sensitivity and low noise of digital cameras made it possible to track the evolution of averaged transverse distributions of a single electron at 6 to 8 points around the IOTA ring, depending on the experiments being carried out at the same time. Fitting the transverse projections of the synchronously captured images gives instantaneous amplitudes of electron oscillations at all 3 degrees of freedom: horizontal, vertical and longitudinal. An analysis of long
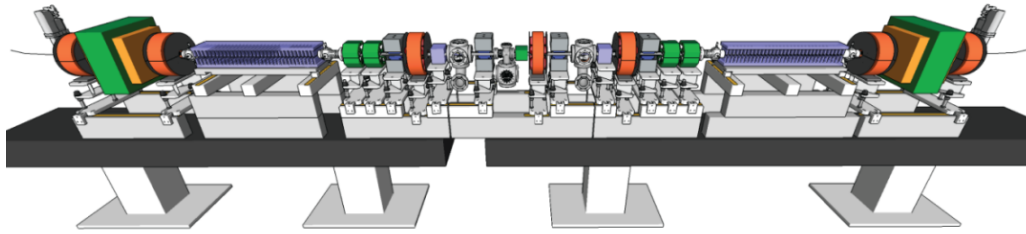
Figure 7: Integrated solid model of the IOTA OSC insertion.

series of electron oscillations under various conditions is being prepared for publication.

NEXT RUNS AT THE IOTA FACILITY

Optical Stochastic Cooling

Optical stochastic cooling (OSC) is a high-bandwidth beam cooling technique that extends the principle of the well-known stochastic cooling to optical frequencies; this represents an increase of three to four orders of magnitude in the achievable state-of-the-art cooling rate [25–27]. IOTA's OSC program will demonstrate the physics of OSC for the first time and use that physics to explore closed-loop interactions of a particle with its own radiation. These investigations will include the rate of energy exchange between the particle and its radiation; the phase-space structure of the cooling force and how it is affected by position and momentum deviations of the particle and nonlinearities in its motion; optical amplification of the radiation and the effects of quantum-mechanical noise on the interaction physics; the interplay between OSC and other beam physics occurring in the ring (IBS, Touschek, residual-gas scattering); and shaping of the cooling force in space and time to provide unprecedented precision and flexibility in phase-space control of the particle(s).

The upcoming OSC experiment will be in the so called "passive" configuration, which does not use optical amplification [28]; however, OSC will still dominate the synchrotron-radiation damping rate by 20-40x. The hardware for this experiment, shown in Figure 7, is currently being aggregated and prepared for installation. To accelerate work, we initially will install a minimal configuration of the magnetic elements and light optics; which excludes the OSC undulators, sextupoles and the optical delay stage. The OSC lattice will be established and corrected, and an existing undulator will be positioned alternately at the pickup and kicker locations for validation of the OSC diagnostics and imaging systems. We will subsequently configure for the full OSC experiment and attempt to demonstrate cooling in Q2 of FY'20. The concept and designs for an OSC experiment with optical amplification are currently under development.

IOTA with Protons

Intensive preparation for the proton program at IOTA is underway in parallel with the preparation for the upcoming runs with electrons. Recommissioned and surplus components from former HINS [29] and FAST projects will be used in the IOTA's proton injector. Table 2 contains the main parameters of IOTA with protons.

Table 2: Proton Beam Parameters

Parameter	Value
LEBT energy	50 keV
MEBT energy	2.5 MeV
Relativistic β	0.073
N_p in IOTA	1×10^{11}
ϵ_x, ϵ_y, RMS	$(3.3, 3.3)\ \mu m$
$\Delta p/p$, RMS	2×10^{-3}

Experiments with intense proton beams at IOTA will require high transmission efficiency from the proton source to IOTA. A LEBT design has been developed that matches the proton source to the RFQ in the transverse plane. Beam parameters from RFQ are known from previous operations and modeling [30]. This data was used to design the MEBT line with beta functions and dispersion matched to those at the injection point in IOTA. The installation of the proton source and injection line will begin at the end of 2019 with the first experiments at IOTA planned for the end of 2020.

Big part of the IOTA's proton program will be dedicated to studies with electron lens that is currently under development. Electron lens allows to form wider range of non-linear potentials by having nondestructive and highly controllable field-forming current distribution overlapped with circulating beam. In addition, the design of the electron lens will be suitable for space-charge compensation studies with electron beam or with trapped secondary electrons and for electron cooling studies [2].

ACKNOWLEDGEMENTS

REFERENCES

[1] V. Danilov and S. Nagaitsev, "Nonlinear accelerator lattices with one and two analytic invariants" *Phys. Rev. ST Accel. Beams*, vol. 13, p. 084002, Aug. 2010.

WEXBA2

[2] S. Antipov *et al.*, IOTA (Integrable Optics Test Accelerator): Facility and experimental beam physics program, *J. Instrum.*, 12, T03002 (2017).

[3] N. Kuklev, Y. K. Kim, S. Nagaitsev, A. L. Romanov, and A. Valishev, "Experimental Demonstration of the Henon-Heiles Quasi-Integrable System at IOTA", in *Proc. IPAC'19*, Melbourne, Australia, May 2019, pp. 386–389. doi:10.18429/JACoW-IPAC2019-MOPGW113

[4] I. Lobach *et al.*, "Study of Fluctuations in Undulator Radiation in the IOTA Ring at Fermilab", in *Proc. IPAC'19*, Melbourne, Australia, May 2019, pp. 777–780. doi:10.18429/JACoW-IPAC2019-MOPRB088

[5] L. Gupta, S. Baturin, Y. K. Kim, and S. Nagaitsev, "Study of Integrable and Quasi-Integrable Sextupole Lattice", in *Proc. IPAC'19*, Melbourne, Australia, May 2019, pp. 371–374. doi:10.18429/JACoW-IPAC2019-MOPGW107

[6] S. Nagaitsev *et al.*, "Experimental Study of a Single Electron in a Storage Ring via Undulator Radiation", in *Proc. IPAC'19*, Melbourne, Australia, May 2019, pp. 781–784. doi:10.18429/JACoW-IPAC2019-MOPRB089

[7] A. L. Romanov *et al.*, "Commissioning and Operation of FAST Electron Linac at Fermilab", in *Proc. IPAC'18*, Vancouver, Canada, Apr.-May 2018, pp. 4096–4099. doi:10.18429/JACoW-IPAC2018-THPMF024

[8] J. P. Edelen, D. T. Abell, D. L. Bruhwiler, N. M. Cook, C. C. Hall, and S. D. Webb, "A Novel S-Based Symplectic Algorithm for Tracking With Space Charge", in *Proc. IPAC'19*, Melbourne, Australia, May 2019, pp. 3279–3282. doi:10.18429/JACoW-IPAC2019-WEPTS068

[9] C. C. Hall, D. L. Bruhwiler, J. P. Edelen, N. Kuklev, A. L. Romanov, and A. Valishev, "First Measurements of Nonlinear Decoherence in the IOTA Ring", in *Proc. IPAC'19*, Melbourne, Australia, May 2019, pp. 3286–3288. doi:10.18429/JACoW-IPAC2019-WEPTS070

[10] K. Hwang, C. E. Mitchell, and R. D. Ryne, "Chaos Indicators for Studying Dynamic Aperture in the IOTA Ring with Protons", in *Proc. IPAC'19*, Melbourne, Australia, May 2019, pp. 3301–3303. doi:10.18429/JACoW-IPAC2019-WEPTS078

[11] N. Kuklev, J. D. Jarvis, Y. K. Kim, A. L. Romanov, J. K. Santucci, and G. Stancari, "Synchrotron Radiation Beam Diagnostics at IOTA - Commissioning Performance and Upgrade Efforts", in *Proc. IPAC'19*, Melbourne, Australia, May 2019, pp. 2732–2735. doi:10.18429/JACoW-IPAC2019-WEPGW103

[12] A. Halavanau *et al.*, "Undulator Radiation Generated by a Single Electron", in *Proc. IPAC'19*, Melbourne, Australia, May 2019, pp. 1867–1870. doi:10.18429/JACoW-IPAC2019-TUPRB089

[13] S. Szustkowski, A. L. Romanov, A. Valishev, S. Chattopadhyay, and N. Kuklev, "Nonlinear Tune-Shift Measurements in the Integrable Optics Test Accelerator", presented at the NAPAC'19, Lansing, MI, USA, Sep. 2019, paper TUZBB6, this conference.

[14] S. A. Antipov, A. Didenko, V.A. Lebedev, and A. Valishev, "Stripline kicker for integrable optics test accelerator", in *Proc. IPAC'15*, Richmond, VA, USA, May 2015, pp. 3390–3392.

[15] N. Kuklev, Y. K. Kim, A. L. Romanov, and A. Valishev, "Experimental Studies of Single Invariant Quasi-Integrable Nonlinear Optics at IOTA", presented at the NAPAC'19, Lansing, MI, USA, Sep. 2019, paper TUPLM08, this conference.

[16] N. Kuklev and Y. K. Kim, "Online Modelling and Optimization of Nonlinear Integrable Systems", presented at the NAPAC'19, Lansing, MI, USA, Sep. 2019, paper TUYBB4, this conference.

[17] N. Eddy *et al.*, "Demonstration of improved transverse stability in the IOTA storage ring via non-linear focusing of the octupole strings", to be submitted to PRAB.

[18] I. Lobach, V. Lebedev, S. Nagaitsev, A. L. Romanov, G. Stancari, A. Halavanau, Z. Huang, and K.-J. Kim, "Intensity Fluctuations in Undulator Radiation", to be submitted to PRAB.

[19] I. Lobach *et al.*, "Study of Fluctuations in Undulator Radiation in the IOTA Ring at Fermilab", presented at the NAPAC'19, Lansing, MI, USA, Sep. 2019, paper THYBA5, this conference.

[20] M. C. Teich, T. Tanabe, T. C. Marshall, and J. Galayda, "Statistical properties of wiggler and bending-magnet radiation from the Brookhaven Vacuum-Ultraviolet electron storage rin" *Phys. Rev. Lett.*, vol. 65, p. 3393, DEC. 1990.

[21] S. C. Gottschalk, R. N. Kelly, M. A. Offenbacker, and J. F. Zumdieck, "Design and performance of the NLCTA-Echo 7 undulator", in *Proc. FEL'12*, Nara, Japan, Aug. 2012, paper THPD12, pp. 571-574.

[22] K.-J. Kim, Z. Huang, and R. Lindberg, "Synchrotron radiation and free-electron lasers" *Cambridge university press*, 2017.

[23] L. V. Pinayev, V. M. Popik, T. V. Shaftan, A. S. Sokolov, N. A. Vinokurov, and P. V. Vorobyov, "Experiments with undulator radiation of a single electron", *Nucl. Instr. and Meth.*, A 341, pp. 17–20, 1994.

[24] A. N. Aleshaev, I. V. Pinayev, V. M. Popik, S. S. Serednyakov, T. V. Shaftan, A. S. Sokolov, N. A. Vinokurov, and P. V. Vorobyov, "A study of the influence of synchrotron radiation quantum fluctuations on the synchrotron oscillations of a single electron using undulator radiation", *Nucl. Instr. and Meth.*, A 359, pp. 80–84, 1995.

[25] S. van der Meer, "Stochastic damping of betatron oscillations in the ISR", CERN-ISR-PO-72-31, 1972.

[26] A. A. Mikhailichenko, M. S. Zolotorev, "Optical stochastic cooling", *Phys. Rev. Lett.* 71 (25), p. 4146, 1993.

[27] M. S. Zolotorev, A. A. Zholents, "Transit-time method of optical stochastic cooling", *Phys. Rev. E* 50 (4), p. 3087, 1994.

[28] J. D. Jarvis *et al.*, "Optical Stochastic Cooling Program at Fermilab's Integrable Optics Test Accelerator", presented at the NAPAC'19, Lansing, MI, USA, Sep. 2019, paper TUPLM21, this conference.

[29] G. W. Foster and J. A. MacLachlon, "An Multi-Mission 8 GeV Injector Linac As A Fermilab Booster Replacement", in *Proc. LINAC'02*, Gyeongju, Korea, Aug. 2002, paper FR202.

[30] P. N. Ostroumov, V. N. Aseev, and A. A. Kolomiets, "Application of a new procedure for design of 325 MHz RFQ", *JINST*, Vol. 1, Apr. 2006.

WEXBA2